Main Manuscript for

Stepwise origin and evolution of a cryptic antimicrobial peptide in mammalian lactoferrin

Titas Sil[1,2], Caitlin H. Kowalski[1,3], Sierra Scamfer[2,4], Matthew F. Barber[1,2,*]

[1]Institute of Ecology and Evolution, University of Oregon; Eugene, OR 97403, USA.

[2]Department of Biology, University of Oregon; Eugene, OR 97403, USA.

[3]Department of Dermatology, Dartmouth Hitchcock Medical Center; Lebanon, NH 03756, USA.

[4]Institute of Molecular Biology, University of Oregon; Eugene, OR 97403, USA.

*corresponding author

Email: mfbarber@uoregon.edu

Author Contributions:

T.S. and M.F.B. designed research; T.S. performed research; T.S., C.H.K., and S.S. contributed to data collection; T.S. and M.F.B. wrote the paper; T.S., C.H.K., S.S., and M.F.B edited the paper.

Competing Interest Statement: Authors declare that they have no competing interests.

Classification: Biological Sciences; Evolution

Keywords: protein evolution, antimicrobial peptides, innate immunity, pathogens, lactoferrin

This PDF file includes:

Main Text
Figures 1 to 5

Abstract

Antimicrobial peptides (AMPs) constitute key components of innate immunity across the tree of life. Canonical AMPs are typically translated as small proteins and secreted from host cells to act against microbes. However, cryptic AMP-like domains are also embedded within diverse proteins not classically associated with antimicrobial function. How such embedded AMPs first emerge and diversify remains unclear. Here we retrace the origin and evolution of the abundant mammalian protein lactoferrin and its embedded AMP, lactoferricin. By resurrecting extinct lactoferrin ancestors dating back to the earliest mammals, we identify a gradual enrichment of cationic and hydrophobic amino acids in the lactoferricin domain over time. These changes enabled ancient lactoferricin to first rupture bacterial membranes, an activity that was later enhanced in extant mammals conferring potent bactericidal activity against diverse bacteria. In

addition, we find that recent natural selection within the lactoferricin domain has continued to modulate antimicrobial activity on recent evolutionary timescales. In particular, we pinpoint a single rapidly evolving site in lactoferricin among great apes that significantly enhances antimicrobial potency against major pathogenic bacteria. Together our study illustrates how novel immune protein functions can arise, evolve, and diversify to strengthen host defense against diverse microbial pathogens.

Main Text

Introduction

The evolution of immune function is vital for species survival in response to pathogen antagonism [1–3]. Antimicrobial peptides (AMPs), also known as host defense peptides, are major contributors to innate immunity across all domains of life, displaying a range of antimicrobial and immunomodulatory activities [4–7]. Well-characterized AMPs are typically small (less than 50 amino acids) and positively charged, promoting interactions with negatively charged microbial cell envelopes [4,5,8]. These interactions can lead to membrane disruption, cell lysis, and impairment of essential cellular processes, ultimately inhibiting microbial growth or triggering cell death [8]. Beyond canonical AMPs, an increasing number of studies have identified the presence of AMP-like domains embedded within larger proteins [9–13]. These domains can in some cases be liberated through proteolytic cleavage, suggesting a mechanism by which diverse proteins may acquire immune functionality. At present, little is known regarding the origins of these embedded AMP domains or the molecular changes that enabled the acquisition of antimicrobial activity.

The mammalian protein lactoferrin provides an exemplar for the evolution of antimicrobial functions. Lactoferrin is an abundant secreted iron-binding protein that arose by duplication of the transferrin gene in the ancestor of placental mammals approximately 160 million years ago (Fig. S1A) [14,15]. Transferrin proteins are typically composed of two homologous domains, termed the N- and C-lobes, each of which binds a single ferric iron ion with high affinity [15–18]. Serum transferrin mediates iron transport in the bloodstream, delivering this essential metal nutrient to cells via receptor-mediated endocytosis [15]. Transferrin family proteins can also provide a defensive benefit by sequestering iron from invasive pathogens, a process termed “nutritional immunity”[19–21]. Lactoferrin, in contrast to transferrin, is abundantly expressed in mammalian milk, colostrum, tears, secondary granules of neutrophils, and other body fluids [22,23]. Since its birth and divergence, lactoferrin has also acquired novel antimicrobial functions which are absent in extant transferrin (Fig. S1A-B) [23]. The N-terminal region of the lactoferrin N-lobe can be proteolytically cleaved by abundant host proteases such as pepsin, trypsin, and chymotrypsin to generate cationic AMPs, including lactoferricin and lactoferrampin [24–29]. These peptides are capable of killing diverse bacterial and fungal pathogens as well as inhibiting microbial biofilm formation [26,29–32]. Lactoferrin-derived AMPs share key features with conventional AMPs, including a high proportion of positively charged and hydrophobic amino acids that confer amphipathic properties (Fig. 1A, S2A). Despite its functional importance, the evolutionary origin of antimicrobial activity within the lactoferricin domain remains poorly understood. Previously we found that lactoferricin exhibits evidence of repeated positive selection in simian primates, with codons possessing an elevated rate of non-synonymous to synonymous substitutions (dN/dS) [33]. This suggests that lactoferricin has continued to diversify within mammals since the acquisition of antimicrobial activity. Determining how this novel function arose and subsequently evolved in an otherwise well-conserved iron-transport protein could offer broader insights into the origin of antimicrobial proteins and the mechanisms by which new biological functions arise. Here we retrace the stepwise emergence of lactoferricin antimicrobial activity in ancestral mammals, as well as

demonstrate how recent natural selection has enhanced the function of this abundant host defense protein.

Results

Ancestral lactoferrin accumulated positive charges after gene duplication

To investigate the origin and evolutionary history of the lactoferricin domain, we first compared lactoferricin sequences across diverse mammals (Fig. S2A). Given that lactoferricin peptides have been reported of different lengths in different species, we focused our studies on the core 25 amino acids conserved across lactoferricin orthologs (amino acids 17-42 in mature human lactoferrin) [24,25]. Most homologs possessed elevated isoelectric points indicating enrichment of positively charged amino acids such as arginine (R), lysine (K), and histidine (H). They also contained interspersed hydrophobic residues characteristic of AMPs. Despite these conserved physiochemical properties, lactoferricin amino acid sequences were highly diverse across orthologs, making it difficult to pinpoint amino acids that may have been responsible for antimicrobial function (Fig. S2A).

To retrace the mutations that led to the emergence of a novel antimicrobial function, we reconstructed ancestral lactoferrin and transferrin sequences across diverse mammals (Fig. 1B). Ancestral sequence reconstruction provides a powerful approach to characterize the function of ancient proteins [34–36]. Using the Topiary software pipeline [37] and publicly available transferrin and mammalian lactoferrin sequences from NCBI, we predicted ancestral amino acid sequences of transferrin and lactoferrin proteins (Fig. S2B). We focused on ancestral proteins (prefixed “Anc”) at key nodes of the phylogenetic tree where the lactoferricin domain underwent significant divergence (Fig. 1B-C). Each predicted sequence was associated with posterior probability scores, which identified the most likely residue at each site as well as the most probable alternative (Fig. S3). These data were used to generate corresponding alternative (Altall_Anc) peptide sequences, in which alternative amino acid states with a posterior probability greater than 0.2 replaced the most probable ancestral amino acid. To assess the robustness of our findings, we included both the primary ancestral reconstructions and their alternate versions in subsequent functional analyses (Fig. S4).

To compare the antimicrobial function of lactoferricin between ancestral and extant variants, we chose human and bovine lactoferrin (hLF and bLF, respectively) as extant references, given the extensive previous work on these orthologs in the field [22,24,25,27]. As a negative control we selected human serum transferrin (hTF) as it did not exhibit antimicrobial function in the N-terminal region (Fig. S1B). We referred to the last common ancestor of mammalian transferrin prior to the gene duplication event as AncTF. Gene duplication produced the first ancestral lactoferrin, which we designated AncLF1 (Fig. 1B). We also considered two intermediate ancestors, denoted AncLF2 and AncLF3. AncLF2 represents the last common ancestor of hLF and bLF in the gene phylogeny, and AncLF3 represents a bovine-specific ancestor that accumulated multiple substitutions in the lactoferricin region relative to AncLF2 (Fig. 1C). We then predicted the structures of these full-length ancestral proteins using AlphaFold2 (Fig. 1B). When the surface electrostatic potentials were compared, we observed a progressive increase in positive charge density (blue surface) in the N-terminal region of lactoferrin following the duplication event (Fig. 1B). This suggests that the emergence of positively charged surfaces in the N-terminus occurred shortly before or after the origin of lactoferrin itself in placental mammals.

We next examined the lactoferricin domains of these reconstructed lactoferrin ancestors, which we refer to as AncLFcin1, AncLFcin2, and AncLFcin3 (Fig. 1C). As the corresponding region in transferrin (residues 17-42) does not form a known antimicrobial peptide, we referred to these homologous sequences as AncTF17-42 in ancestral transferrin and hTF17-42 in human serum transferrin. We observed that cationic amino acids became more abundant in lactoferricin post-duplication, with the emergence of a K5 substitution in AncLFcin1, R8 in AncLFcin2, and R9 in AncLFcin3 (Fig. 1C). To quantify this trend, we calculated peptide isoelectric points, which

143 increased from AncTF17-42 to bLFcin (Fig. 1C). Furthermore, we noted the emergence of
144 hydrophobic residues adjacent to positively charged amino acids in the lactoferricin domain after
145 duplication (e.g., alanine 1 in AncLFcin1 and AncLFcin2). Based on these observations, we
146 hypothesized that the increase in positive charge and hydrophobicity enabled lactoferricin to
147 acquire antimicrobial function by mediating association with bacterial cell envelopes.
148
149 ***Early origin of antimicrobial activity in lactoferricin***
150 To characterize the antimicrobial potency of ancestral and extant lactoferricin domains, we
151 synthesized these peptides and tested their activity against several bacterial pathogens (Fig. 2).
152 Among Gram-negative bacteria we included *Pseudomonas aeruginosa*, a pathogen frequently
153 associated with nosocomial infections, chronic wounds, and cystic fibrosis, as well as a reference
154 strain of the enteric bacterium *Escherichia coli* [38–40]. We also tested representative Gram-positive
155 bacteria including *Staphylococcus aureus*, a major cause of invasive hospital and community-
156 acquired infections, as well as *Streptococcus agalactiae*, a frequent agent of severe infections in
157 neonates [41–43].
158
159 To compare the antimicrobial potency of ancestral and extant lactoferricin homologs, we
160 measured bacterial growth in presence of the peptides at various concentrations over 24 hours.
161 Human lactoferrin concentrations range widely *in vivo* from 7-8 mg/mL in colostrum, 1-3 mg/mL in
162 breast milk, 0.1-2 mg/mL in tears and saliva, and even lower levels (0.001-0.1 mg/mL) in other
163 secretory body fluids [44]. We therefore used physiologically relevant concentrations of each
164 peptide, ranging from 0.1-1mg/mL, to assess their dose-dependent antimicrobial activities.
165 Bacterial growth at each concentration was measured by normalized area under the curve (AUC)
166 calculations, where higher AUC corresponds to increased bacterial growth. Relative to the
167 untreated control, peptides exhibiting <50% bacterial growth were classified as having high
168 antimicrobial potency, those with 50–75% growth as moderate, and those with >75% growth as
169 weak. We observed that all bacteria grew to high levels in the presence of hTF17-42, indicating it
170 has little to no antimicrobial activity as expected (Fig. 2). Similarly, the ancestral-derived peptide
171 AncTF17-42 exhibited negligible antimicrobial activity across all doses and pathogens (Fig. 2).
172 AncLFcin1, in contrast, reduced growth by >50% at higher doses against a subset of pathogens,
173 for example at 400 µg/mL against *P. aeruginosa* PAO1 and at 800 µg/mL against *E. coli* (Fig. 2A-
174 B). These findings suggest that antimicrobial activity in this domain arose after the gene
175 duplication event that gave rise to mammalian lactoferrin.
176
177 AncLFcin2, representing the last common ancestor of hLF and bLF, exhibited higher potency at
178 lower concentrations across all pathogens tested relative to AncLFcin1 (Fig. 2). For example, it
179 was highly potent at 100 µg/mL against *P. aeruginosa* PAO1, and at 50 µg/mL against *E. coli* and
180 *S. aureus* MN8 (Fig. 2A, 2C, 2E). Against other pathogens, AncLFcin2 also reduced bacterial
181 growth by >50% in the 100-400 µg/mL range. These results suggest that antimicrobial activity of
182 the lactoferricin domain was substantially enhanced between AncLFcin1 and AncLFcin2.
183 AncLFcin3 exhibited broad antimicrobial activity in the 100-800 µg/mL range but overall was less
184 effective than bLFcin. To validate the robustness of our ancestral sequence reconstruction, we
185 also tested alternate versions of each ancestor against *P. aeruginosa* and *S. aureus* (Fig. S4).
186 Overall trends in antimicrobial activity were largely consistent with those observed for the primary
187 reconstructed ancestors. The only exception was Altall_AncTF17-42, which exhibited weak
188 activity against *S. aureus* at the highest concentrations (Fig. S4).
189
190 Among extant lactoferricin orthologs, bLFcin was consistently more potent than hLFcin against all
191 pathogens tested, significantly reducing bacterial growth at concentrations as low as 50 µg/mL
192 (Fig. 2). Notably, hLFcin was more effective against Gram-negative bacteria where it restricted
193 growth at 100-200 µg/mL. Against Gram-positive bacteria, the antimicrobial potency of hLFcin
194 only became evident at concentrations above 200 µg/mL. Interestingly, AncLFcin2 was more
195 effective than hLFcin against Gram-positive bacteria. Overall these data indicate that modest
196 antimicrobial activity first emerged in AncLFcin1, immediately after the emergence of lactoferrin in
197 ancient mammals, which then increased in subsequent ancestors. However, given that hLFcin
198 exhibited weaker antimicrobial activity than some earlier ancestors, our findings also suggest that

199 the evolution of lactoferricin antimicrobial function did not increase uniformly during mammalian
200 evolution.
201
202 ***Stepwise enhancement of bactericidal activity during lactoferricin evolution***
203 After broadly characterizing the antimicrobial nature of the ancestral and extant lactoferricins, we
204 assessed their function in greater detail by measuring growth kinetics and viability of
205 representative Gram-negative (*P. aeruginosa*) and Gram-positive (*S. aureus*) bacteria in the
206 presence of the peptides (Fig. 3). In addition to analysing growth curves and calculating AUCs,
207 we quantified bacterial survival by measuring colony-forming units (CFUs) over time. Based on
208 the differences in dose-dependent activity observed previously, we used 100 µg/mL of the
209 peptides against *P. aeruginosa* and 800 µg/mL against *S. aureus* in subsequent experiments.
210
211 Consistent with our previous results, extant and ancestral transferrin-derived peptides, hTF17-42
212 and AncTF17-42 respectively, exhibited no detectable effects on *P. aeruginosa* growth and
213 survival (Fig. 3A–C). AncLFcin1 displayed an intermediate phenotype, with a modest but
214 significant reduction in overall *P. aeruginosa* growth (Fig. 3A, B). We also observed a rapid
215 decrease in *P. aeruginosa* viability within 2 hours of treatment, followed by a partial recovery (Fig.
216 3C). In contrast, AncLFcin2 consistently suppressed *P. aeruginosa* growth throughout the
217 experiment, resulting in a significant 1000-fold reduction in bacterial viability after 24 hours of
218 treatment (Fig. 3A-C). AncLFcin3, the ancestor of bLFcin, inhibited *P. aeruginosa* growth and
219 caused 100-1000 fold reduction in viability during the first 15 hours of treatment, after which
220 bacterial growth resumed. hLFcin also consistently suppressed *P. aeruginosa* growth, causing a
221 10,000 fold reduction in viability at the end of the treatment. Finally, bLFcin exhibited the most
222 potent bactericidal effect, reflected by minimal AUC values and no detectable *P. aeruginosa*
223 colonies within 2 hours of treatment (Fig. 3A-C).
224
225 Lactoferricin activity profiles against *S. aureus* differed from those of *P. aeruginosa* in several
226 ways (Fig. 3D–F). hTF17-42 and AncTF17-42 exhibited modest inhibitory effects on *S. aureus*
227 later in the treatment period (Fig. 3D, E), but these differences did not translate into reductions in
228 bacterial viability as measured by CFU counts (Fig. 3F). AncLFcin1 exerted partial inhibition
229 against *S. aureus,* with little reduction in bacterial viability. AncLFcin2 strongly suppressed
230 bacterial growth, resulting in an approximately 100,000 fold reduction in *S. aureus* viability by the
231 end of treatment. AncLFcin3 also significantly inhibited *S. aureus* growth and reduced its viability
232 over the course of the experiment. In contrast, hLFcin initially inhibited bacterial growth and
233 caused a rapid 100-fold reduction in viability. Subsequently, *S. aureus* resumed growth, although
234 this was not reflected in the optical density, possibly due to a reduction in cell size. Again, bLFcin
235 remained the most potent peptide, eliminating detectable colonies within two hours (Fig. 3F).
236 Collectively these findings indicate that weak antimicrobial activity emerged in the earliest
237 lactoferricin ancestor, with bactericidal activity substantially enhanced in subsequent orthologs.
238
239 ***Lactoferricin membrane permeabilizing activity arose early after gene birth***
240 While both ancestral and extant lactoferricin peptides exhibited some degree of bactericidal
241 activity, they varied dramatically in their potency (Fig. 3). This led us to further examine the
242 molecular mechanisms underlying differences in their activities. A common feature of many
243 cationic AMPs is their ability to disrupt and permeabilize bacterial membranes [4,6]. To investigate
244 this function, we measured the membrane permeabilizing ability of ancestral and extant
245 lactoferricin peptides against *P. aeruginosa*. Membrane permeabilization was measured by
246 staining with propidium iodide (PI) which enters the bacterial cell and binds DNA only when cell
247 membranes are compromised [45]. We found that all ancestral and extant lactoferricins, but not
248 transferrin-derived peptides, were capable of permeabilizing bacterial membranes within 30
249 minutes of incubation as detected by PI staining (Fig. 4A). This finding indicates that bacterial
250 membrane permeabilization was an early trait that emerged in the lactoferricin domain shortly
251 after gene duplication.
252
253 Membrane permeabilization by AMPs can induce bacterial stress responses as well as alter
254 membrane polarization and ion flux, which in turn impacts cell physiology and morphology [46,47].

255 To determine the extent to which ancestral and extant lactoferricins affect target cell physiology,
256 we measured bacterial membrane polarization. *P. aeruginosa* cells were treated with the cationic
257 dye 3,3'-dipropylthiadicarbocyanine iodide ($DiSC_3(5)$) that accumulates in polarized membranes
258 quenching its fluorescence [48]. Upon membrane depolarization, $DiSC_3(5)$ is released, and
259 fluorescence increases. We found that all ancestral and extant lactoferricin-treated cells were
260 hyperpolarized, as demonstrated by a reduction in fluorescence, compared to untreated, hTF17-
261 42, or AncTF17-42-treated cells (Fig. 4B).
262
263 Given that all lactoferricin peptides exhibited both membrane-permeabilizing and polarization-
264 altering activities, we sought to understand how these peptides nonetheless differed in their
265 overall antimicrobial potency. To address this, we shifted from population-level assays to single-
266 cell morphological characterization. We hypothesized that lactoferricin variants with increased
267 antimicrobial activity would exert greater impact on bacterial cell envelope integrity. To visualize
268 this, we treated *P. aeruginosa* with the lipophilic dye Nile red, which homogenously binds to
269 membranes and produces brightly stained foci in regions of increased fluidity, indicative of
270 membrane perturbation[45]. Using spinning-disc confocal microscopy, hTF17-42 and AncTF17-42
271 exhibited no visible effects on bacterial morphology (Fig. 4C). In contrast, cells treated with
272 AncLFcin1, AncLFcin2, or AncLFcin3 displayed puncta-like structures on their membranes,
273 suggesting localized membrane disturbance. These cells also appeared significantly smaller than
274 untreated controls. This effect was most pronounced with hLFcin and bLFcin, where cells became
275 markedly reduced in size, rounded, and membranes were barely distinguishable from the cytosol
276 (Fig. 4C). Quantitative measurements of cell size confirmed that ancestral lactoferricins induced
277 moderate but significant cell shrinkage, whereas extant variants amplified this effect (Fig. 4D).
278
279 Membrane disruption is a common mechanism of AMP function, which can cause leaking of
280 cytoplasmic content and shrinkage of cells [45,49,50]. Such perturbations can be transient and
281 resealable or irreversible, depending on the extent of the damage [50,51]. Our results suggest that
282 bacteria are able to recover from ancestral lactoferricin-induced membrane damage, whereas
283 extant variants, particularly bLFcin, caused irreversible cell envelope collapse. Together, these
284 findings indicate that the lactoferricin domain initially possessed membrane-permeabilizing
285 activity, which intensified during evolution to produce potent bactericidal effects.
286
287 ***Rapid evolution of lactoferricin antimicrobial activity in primates***
288 In addition to investigating the molecular origins of the lactoferricin domain, we also sought to
289 determine how lactoferricin antimicrobial activity has changed over recent evolutionary
290 timescales. Previous work by our group found evidence that lactoferrin has been subject to
291 repeated positive selection within human populations as well as between simian primate species,
292 suggesting antimicrobial activity may have been modulated via recurrent adaptation [18,33]. We
293 identified several sites in the N-lobe of lactoferrin with elevated rates of nonsynonymous to
294 synonymous substitutions (dN/dS), including two within the lactoferricin region (Fig. 5A, S5) [33].
295 For example, position 5 varies between primates, with humans and many monkeys encoding a
296 glutamine (Q), whereas all other great apes encode an arginine (R). In addition, position 12 is
297 variable among primates as well as polymorphic within human populations, generally toggling
298 between cationic arginine and lysine (K12 or R12) residues [33].
299
300 To assess the functional consequences of natural selection at sites 5 and 12, we generated two
301 point mutants in human lactoferricin: hLFcinK12R and hLFcinQ5R. hLFcinK12R exhibited
302 antimicrobial activity comparable to wild type hLFcin against both *P. aeruginosa* and *S. aureus,*
303 indicating that the K12R substitution does not substantially alter activity against these pathogens
304 (Fig. 5B, C). In contrast, the hLFcinQ5R mutant displayed significant enhancement in
305 antimicrobial potency against *S. aureus* relative to hLFcin (Fig. 5B, C). Beyond the addition of a
306 single positive charge, this effect may stem from the positioning of R5 adjacent to the aromatic
307 hydrophobic residue tryptophan (W6). We noted a similar pattern in AncLFcin2, which exhibited
308 greater potency against *S. aureus* than hLFcin and contains a lysine (K5) adjacent to
309 phenylalanine, another aromatic hydrophobic residue (Fig. 1C, 2C-D, 3D-F). Notably, the most
310 potent variant, bLFcin, contains both combinations, which may contribute to its heightened

311 antimicrobial activity. Taken together, these findings indicate that antimicrobial function of the
312 lactoferricin domain has been repeatedly modulated by the forces of natural selection, leading to
313 enhanced activity across mammalian lineages.
314
315 **Discussion**
316
317 AMPs have long been appreciated as deeply conserved effectors of innate immunity. Recent
318 large-scale analyses further suggest that AMP-like domains are far more widespread than
319 previously appreciated [10–13]. Computational studies have detected AMP-like domains embedded
320 within diverse proteins not previously associated with direct antimicrobial function, including
321 interferon gamma, IL-13, histone H1, gasdermin E, and dynactin, among others [10–13]. The
322 existence of such cryptic antimicrobial functions suggests a previously unappreciated layer of
323 host defense, though the evolutionary origins of such embedded AMPs remain largely
324 uncharacterized. Leveraging mammalian lactoferrin and its embedded AMP lactoferricin as a
325 model, we observed that even the earliest lactoferricin ancestor possessed the ability to
326 permeabilize bacterial membranes and alter membrane potential, a property that was further
327 enhanced in later ancestors (Fig. 4). This increased activity was accompanied by a marked
328 perturbation of bacterial cells, likely due to leakage of cytoplasmic content [49–51]. Membrane
329 permeabilization by AMPs is often reversible depending on the severity of damage [50,51]. Hence, it
330 is reasonable to speculate that early lactoferricin domains induced perturbations that bacteria
331 could repair, allowing eventual recovery. In contrast, more potent lactoferricin variants such as
332 bLFcin induced irreversible damage at much lower concentrations, leading to complete lysis or
333 severe morphological damage that prevented recovery (Fig. 4). These findings demonstrate that
334 membrane permeabilization and hyperpolarization were early antimicrobial traits of lactoferricin,
335 and that bactericidal activity intensified over time. Assessing the activity of additional lactoferricin
336 ancestors or mutants could aid in further resolving the molecular basis of this activity in future
337 work.
338
339 We noted that some ancestral lactoferricins exerted higher antimicrobial activity than their extant
340 orthologs. For example, AncLFcin2 and AncLFcin3 were consistently more bactericidal against *S.*
341 *aureus* than human lactoferricin (Fig. 2, 3). Thus, the evolution of antimicrobial function in
342 lactoferrin does not reflect a simple linear increase in potency but has rather fluctuated along
343 different lineages depending on the target microbe. We considered whether a reduction in
344 lactoferricin antimicrobial activity could indicate a trade-off to minimize toxicity against host cells.
345 However, treatment of bovine erythrocytes revealed no significant hemolysis in the presence of
346 any lactoferricin peptides, inconsistent with this hypothesis (Fig. S6). An alternative explanation is
347 that some bacteria may have evolved host-specific resistance to these AMPs. *S. aureus*, for
348 example, is human associated with many of its virulence factors and toxins exhibiting narrow
349 tropism for humans [52–54]. Alternatively, trade-offs with antimicrobial activity could arise due to
350 other factors such as peptide stability, ease of protease digestion, or iron binding ability of the N-
351 lobe. In addition, this study was performed in a low-nutrient laboratory media which do not fully
352 recapitulate the host environment. Future studies could measure the activity of lactoferricin
353 variants in alternative host-mimicking conditions or *in vivo*, which may reveal as-yet unknown
354 impacts on antimicrobial function. Together these results underscore how ancestral sequence
355 reconstruction can uncover unique variants of extant AMPs that could serve as safe and effective
356 pathogen treatment options, particularly in the era of growing antibiotic resistance [5,55].
357
358 AMPs have frequently been identified among the most rapidly evolving genes in host genomes,
359 likely reflecting repeated adaptation to counteract diverse microbes [56,57]. In contrast, far less is
360 known about how AMP domains embedded within larger proteins emerge and evolve in response
361 to selection. We previously identified two sites exhibiting signatures of positive selection in the
362 lactoferricin domain among primates [33]. Notably, one of these substitutions (Q5R) was sufficient
363 to significantly enhance the antimicrobial activity of human lactoferricin, particularly against *S.*
364 *aureus* (Fig. 5). This observation suggests the importance of this region for lactoferricin's activity.
365 Notably, the adjacent sixth residue is invariably an aromatic hydrophobic amino acid, either
366 phenylalanine (F) or tryptophan (W), across all lactoferricin sequences (Fig. 1C). AncLFcin2,

which is effective against all pathogens tested, also possesses cationic and aromatic hydrophobic residues at these sites (K5F6). The most potent variant tested, bovine lactoferricin, contains three such pairs of cationic and aromatic residues (F1K2, R5W6, and W7R8). Although hTF and AncTF both contain a F6R7 amino acid pair, the effect of the positively charged arginine is likely diminished by the neighboring aspartate (D8). Given that cationic nature and hydrophobicity are key features of many AMPs, the juxtaposition of a cationic residue with an aromatic hydrophobic residue within lactoferrin may reflect positive epistasis between these sites. Indeed, epistasis between nearby R and W residues has been reported previously in antiviral proteins [58]. It is well established that cationic amino acids mediate electrostatic interactions with the negatively charged bacterial envelopes, whereas hydrophobic residues insert into membranes and contribute to disruption of the lipid bilayer [59]. Future work could determine how selection and epistasis together contribute to antimicrobial potency in these and other AMPs.

It is notable that lactoferrin has been reported to contain not just one, but multiple embedded antimicrobial domains. For example, the lactoferrin N-lobe contains a 17-amino acid region termed lactoferrampin that possesses antimicrobial activity against both bacteria and fungi [60]. In addition, ovotransferrin, the ortholog of mammalian transferrin in birds, has also been reported to contain an antimicrobial fragment within the N-lobe in a region distinct from both lactoferricin and lactoferrampin [61,62]. These observations suggest that embedded AMPs may have arisen multiple times within lactoferrin or transferrin homologs during the course animal evolution. This protein family could thus provide an informative system to further investigate the origins and evolution of antimicrobial functions.

In addition to providing protection against invasive pathogens, the expression of AMPs at barrier tissues positions them to broadly shape host-associated microbiotas. Work in *Drosophila* has demonstrated how natural selection and polymorphism in AMP genes can impact diverse resident microbes [56,63,64], as well as confer defense against microbes within specific ecological niches [65]. Given that lactoferrin is among the most abundant secreted proteins in many mammalian barrier tissues, genetic variation may similarly shape the diversity and composition of host-associated microbial communities. By retracing the origin and evolution of antimicrobial activity in mammalian lactoferrin, our study illustrates how new protein functions can emerge to promote host defense against major microbial pathogens.

Materials and Methods

Ancestral sequence reconstruction

Vertebrate transferrin and mammalian lactoferrin homologs were retrieved from the NCBI and UniProt databases for ancestral sequence reconstruction. Multiple sequence alignments and maximum likelihood phylogenetic trees were generated using the Topiary pipeline [37]. Alignments were manually scanned to remove insertions and deletions. Using Topiary, ancestral sequences were inferred at each node, with posterior probabilities calculated for each site and node to assess reconstruction confidence.

Peptide synthesis

All peptides were commercially synthesized by GenScript. Lyophilized peptides were resuspended in phosphate-buffered saline (PBS, pH 7.0) to a concentration of 10 mg/mL and stored at –80°C.

Structural prediction of ancestral sequences

Protein structure predictions for the reconstructed ancestral sequences were performed using ColabFold, a streamlined implementation of AlphaFold2[66]. Prior to structure prediction, the N-terminal region corresponding to the human lactoferrin signal peptide (hLF1–19) was removed from all ancestral sequences. Predicted protein structures were visualized and analyzed using UCSF ChimeraX (version 1.8, released 2024-06-10)[67]. The theoretical isoelectric point (pI) of each peptide was calculated using the ExPASy Compute pI/Mw tool[68].

423
424 **Bacterial growth assays**
425 Overnight cultures of all bacterial strains were prepared by inoculating a single colony into low-
426 nutrient 5% tryptic soy broth (TSB, v/v) to model the low-nutrient conditions of the host
427 environment (*5*) and incubated at 250 rpm overnight, unless otherwise specified. The following
428 day, cultures were diluted to an optical density at 600 nm (OD_{600}) of 0.02 in fresh 5% TSB. For
429 growth assays, 150 µL of the diluted culture was added to each well of a 96-well microtiter plate,
430 followed by the addition of peptides at the desired concentrations. Plates were incubated for 24
431 hours with continuous shaking in a Synergy H1 microplate reader (BioTek), and bacterial growth
432 was monitored by measuring OD_{600} at 10-minute intervals. Bacterial growth was then normalized
433 by subtracting the optical densities of similar volume of media with or without the peptides of
434 particular concentrations from those of bacterial cultures. Area under the curve (AUC) was
435 calculated and normalized on GraphPad Prism software. For normalization of the AUCs, 100%
436 was defined as the average measurements from the bacterial growth without any peptide added.
437
438 **Bacterial survival assay**
439 Overnight cultures were diluted to an OD_{600} of 0.02 in fresh medium, and antimicrobial peptides
440 were added at the indicated concentrations in 1.5 mL microcentrifuge tubes. To assess bacterial
441 viability over time, samples were taken at defined time points during the treatment period. At each
442 time point, cultures were serially diluted 10-fold (up to 10^{-7}) and plated on tryptic soy agar (TSA)
443 to enumerate colony-forming units (CFUs). Plates were incubated at 37°C overnight, and CFUs
444 were counted the following day to evaluate the time-course of bacterial survival.
445
446 **Membrane permeabilization measurements**
447 Overnight cultures of *Pseudomonas aeruginosa* PAO1 were subcultured by diluting to an OD_{600}
448 of 0.3 in fresh 5% TSB. Aliquots of 100 µL were transferred into 1.5 mL microcentrifuge tubes and
449 treated with the peptides for 30 minutes. Cells were pelleted by centrifugation at 5,000 × g for 1
450 minute. Pellets were resuspended in 300 µL of 20 µM propidium iodide (Sigma-Aldrich P4170-
451 10MG) and incubated in the dark for 15 minutes to prevent photobleaching. Excess dye was
452 removed by centrifugation at 5,000 × g for 1 minute, the supernatant was discarded, and pellets
453 were resuspended in 300 µL of phosphate-buffered saline (PBS, pH 7.0). For fluorescence
454 measurement, 100 µL aliquots from each sample were transferred in triplicate into black-walled,
455 clear-bottom 96-well plates (without lids). Fluorescence intensity was measured from the bottom
456 of the plate using a microplate reader with excitation at 535 nm and emission at 617 nm.
457
458 **Membrane potential measurements**
459 The membrane depolarizing activity of peptides was assessed using the voltage-sensitive dye
460 $DiSC_3(5)$ (MedChem Express #HY-D0085-25mg) as previously described[48]. *Pseudomonas*
461 *aeruginosa* PAO1 overnight cultures were diluted in fresh 5% TSB to OD_{600} of 0.3. $DiSC_3(5)$[48],
462 prepared as a stock solution in DMSO, was added to the bacterial suspension at a final
463 concentration of 5 µM. Following a brief equilibration period to allow dye accumulation across
464 polarized membranes, peptides were added at a final concentration of 100 µg/mL in a black,
465 clear-bottom 96-well plate. Fluorescence was monitored kinetically over a 1-hour period at 37 °C
466 using a Synergy H1 microplate reader (BioTek), with excitation and emission wavelengths set to
467 610 nm and 660 nm, respectively. A decrease in fluorescence intensity was interpreted as
468 membrane hyperpolarization, reflecting increased accumulation of the cationic, lipophilic dye
469 within the bacterial cytoplasmic membrane, where self-quenching reduces the overall
470 fluorescence signal.
471
472 **Nile red staining, microscopy and cell size measurements**
473 The Nile red staining protocol was adapted and modified from Dombach *et al.*, 2021[69]. Overnight
474 bacterial cultures were diluted in fresh 5% tryptic soy broth (TSB, v/v) to an optical density at
475 600 nm (OD_{600}) of 0.3. From this, 100 µL aliquots were transferred to 1.5 mL microcentrifuge
476 tubes for peptide treatment. Samples were incubated at 37 °C for 40 minutes with shaking at
477 250 rpm. Following peptide treatment, Nile red (Sigma-Aldrich 72485-100MG) was added to each
478 tube at a final concentration of 10 µg/mL, followed by a 5-minute incubation at 37 °C. Cells were

then fixed by adding paraformaldehyde to a final concentration of 4%, and incubated at room temperature for 10 minutes. After fixation, cells were pelleted by centrifugation at 10,000 × g for 1 minute and resuspended in 10 µL of PBS, pH 7.0. For microscopy, 7 µL of the resuspended cells was applied to a coverslip, overlaid with 0.5% agarose, and gently compressed with a glass slide to immobilize the sample. Imaging was performed using a SoRA spinning disk confocal microscope (Nikon CSU-W1) equipped with a 60X water-immersion objective. Bacterial cell size was measured using the Fiji package of ImageJ software[70].

Hemolysis assay

The hemolysis assay was adapted from Greco *et al.*, 2020[71]. Bovine red blood cells (RBCs) were isolated by centrifuging 1 mL of whole blood at 3000 × *g* for 2 min. The RBC pellet was washed five times with phosphate-buffered saline (PBS) by resuspension and centrifugation until the supernatant was clear, then diluted 1:10 in PBS. In a 96-well plate, 100 µL of the diluted RBC suspension was mixed with each peptide solution (final concentration: 1 mg/mL) and incubated at 37 °C for 1 h. Absorbance was measured at 405 nm using a microplate reader, and the percentage of hemolysis was calculated relative to a positive control (1% Triton X-100).

Acknowledgements

We thank Mike Harms and Jose Sanchez-Borbon for assistance with ancestral sequence reconstruction. We are thankful to the members of Barber lab for their feedback and support, as well as Karen Guillemin, Jarrod Smith, and Melanie Spero for helpful insights and discussion. We thank the Genomics and Cell Characterization Core Facility (GC3F) at UO and Adam Fries for assistance with microscopy.

References

1. Daugherty, M.D., and Malik, H.S. (2012). Rules of engagement: molecular insights from host-virus arms races. Annu. Rev. Genet. *46*, 677–700.

2. Barber, M.F., and Fitzgerald, J.R. (2024). Mechanisms of host adaptation by bacterial pathogens. FEMS Microbiol. Rev. *48*. https://doi.org/10.1093/femsre/fuae019.

3. Pancer, Z., and Cooper, M.D. (2006). The evolution of adaptive immunity. Annu. Rev. Immunol. *24*, 497–518.

4. Oliveira Júnior, N.G., Souza, C.M., Buccini, D.F., Cardoso, M.H., and Franco, O.L. (2025). Antimicrobial peptides: structure, functions and translational applications. Nat. Rev. Microbiol. https://doi.org/10.1038/s41579-025-01200-y.

5. Magana, M., Pushpanathan, M., Santos, A.L., Leanse, L., Fernandez, M., Ioannidis, A., Giulianotti, M.A., Apidianakis, Y., Bradfute, S., Ferguson, A.L., et al. (2020). The value of antimicrobial peptides in the age of resistance. Lancet Infect. Dis. *20*, e216–e230.

6. Lazzaro, B.P., Zasloff, M., and Rolff, J. (2020). Antimicrobial peptides: Application informed by evolution. Science *368*, eaau5480.

7. Hancock, R.E., and Scott, M.G. (2000). The role of antimicrobial peptides in animal defenses. Proc. Natl. Acad. Sci. U. S. A. *97*, 8856–8861.

8. Zasloff, M. (2002). Antimicrobial peptides in health and disease. N. Engl. J. Med. *347*, 1199–1200.

525 9. Kim, H.S., Yoon, H., Minn, I., Park, C.B., Lee, W.T., Zasloff, M., and Kim, S.C. (2000).
526 Pepsin-mediated processing of the cytoplasmic histone H2A to strong antimicrobial peptide
527 buforin I. J. Immunol. *165*, 3268–3274.

528 10. Yount, N.Y., Weaver, D.C., Lee, E.Y., Lee, M.W., Wang, H., Chan, L.C., Wong, G.C.L., and
529 Yeaman, M.R. (2019). Unifying structural signature of eukaryotic α-helical host defense
530 peptides. Proc. Natl. Acad. Sci. U. S. A. *116*, 6944–6953.

531 11. Goldberg, K., Lobov, A., Antonello, P., Shmueli, M.D., Yakir, I., Weizman, T., Ulman, A.,
532 Sheban, D., Laser, E., Kramer, M.P., et al. (2025). Cell-autonomous innate immunity by
533 proteasome-derived defence peptides. Nature. https://doi.org/10.1038/s41586-025-08615-w.

534 12. Marsman, G., Zheng, X., Čerina, D., Lacey, K.A., Liu, M., Humme, D., Goosmann, C.,
535 Brinkmann, V., Harbort, C.J., Torres, V.J., et al. (2024). Histone H1 kills MRSA. Cell Rep.
536 *43*, 114969.

537 13. Torres, M.D.T., Cesaro, A., and de la Fuente-Nunez, C. (2025). Peptides from non-immune
538 proteins target infections through antimicrobial and immunomodulatory properties. Trends
539 Biotechnol. *43*, 184–205.

540 14. Hughes, A.L., and Friedman, R. (2014). Evolutionary diversification of the vertebrate
541 transferrin multi-gene family. Immunogenetics *66*, 651–661.

542 15. Lambert, L.A. (2012). Molecular evolution of the transferrin family and associated receptors.
543 Biochim. Biophys. Acta *1820*, 244–255.

544 16. Haridas, M., Anderson, B.F., and Baker, E.N. (1995). Structure of human diferric lactoferrin
545 refined at 2.2 Å resolution. Acta Crystallogr. D Biol. Crystallogr. *51*, 629–646.

546 17. Yang, N., Zhang, H., Wang, M., Hao, Q., and Sun, H. (2012). Iron and bismuth bound
547 human serum transferrin reveals a partially-opened conformation in the N-lobe. Sci. Rep. *2*,
548 999.

549 18. Barber, M.F., and Elde, N.C. (2014). Escape from bacterial iron piracy through rapid
550 evolution of transferrin. Science *346*, 1362–1366.

551 19. Murdoch, C.C., and Skaar, E.P. (2022). Nutritional immunity: the battle for nutrient metals at
552 the host-pathogen interface. Nat. Rev. Microbiol. https://doi.org/10.1038/s41579-022-00745-
553 6.

554 20. Iatsenko, I., Marra, A., Boquete, J.-P., Peña, J., and Lemaitre, B. (2020). Iron sequestration
555 by transferrin 1 mediates nutritional immunity in Drosophila melanogaster. Proc. Natl. Acad.
556 Sci. U. S. A. *117*, 7317–7325.

557 21. Barber, M.F., and Elde, N.C. (2015). Buried Treasure: Evolutionary Perspectives on
558 Microbial Iron Piracy. Trends Genet. *31*, 627–636.

559 22. García-Montoya, I.A., Cendón, T.S., Arévalo-Gallegos, S., and Rascón-Cruz, Q. (2012).
560 Lactoferrin a multiple bioactive protein: an overview. Biochim. Biophys. Acta *1820*, 226–236.

561 23. Kowalczyk, P., Kaczyńska, K., Kleczkowska, P., Bukowska-Ośko, I., Kramkowski, K., and
562 Sulejczak, D. (2022). The lactoferrin phenomenon-A miracle molecule. Molecules *27*, 2941.

563 24. Bellamy, W., Takase, M., Yamauchi, K., Wakabayashi, H., Kawase, K., and Tomita, M.
564 (1992). Identification of the bactericidal domain of lactoferrin. Biochim. Biophys. Acta *1121*,
565 130–136.

566 25. Sinha, M., Kaushik, S., Kaur, P., Sharma, S., and Singh, T.P. (2013). Antimicrobial
567 lactoferrin peptides: the hidden players in the protective function of a multifunctional protein.
568 Int. J. Pept. *2013*, 390230.

569 26. Ramamourthy, G., and Vogel, H.J. (2021). Antibiofilm activity of lactoferrin-derived synthetic
570 peptides against Pseudomonas aeruginosa PAO1. Biochem. Cell Biol. *99*, 138–148.

571 27. Ohradanova-Repic, A., Praženicová, R., Gebetsberger, L., Moskalets, T., Skrabana, R.,
572 Cehlar, O., Tajti, G., Stockinger, H., and Leksa, V. (2023). Time to kill and time to heal: The
573 multifaceted role of lactoferrin and lactoferricin in host defense. Pharmaceutics *15*.
574 https://doi.org/10.3390/pharmaceutics15041056.

575 28. Nakamura, M., Tsuda, N., Miyata, T., and Ikenaga, M. (2022). Antimicrobial effect and
576 mechanism of bovine lactoferrin against the potato common scab pathogen Streptomyces
577 scabiei. PLoS One *17*, e0264094.

578 29. León-Calvijo, M.A., Leal-Castro, A.L., Almanzar-Reina, G.A., Rosas-Pérez, J.E., García-
579 Castañeda, J.E., and Rivera-Monroy, Z.J. (2015). Antibacterial activity of synthetic peptides
580 derived from lactoferricin against Escherichia coli ATCC 25922 and Enterococcus faecalis
581 ATCC 29212. Biomed Res. Int. *2015*, 453826.

582 30. Fernandes, K.E., and Carter, D.A. (2017). The antifungal activity of lactoferrin and its derived
583 peptides: Mechanisms of action and synergy with drugs against fungal pathogens. Front.
584 Microbiol. *8*, 2.

585 31. Liao, H., Liu, S., Wang, H., Su, H., and Liu, Z. (2019). Enhanced antifungal activity of bovine
586 lactoferrin-producing probiotic Lactobacillus casei in the murine model of vulvovaginal
587 candidiasis. BMC Microbiol. *19*, 7.

588 32. Singh, P.K., Parsek, M.R., Greenberg, E.P., and Welsh, M.J. (2002). A component of innate
589 immunity prevents bacterial biofilm development. Nature *417*, 552–555.

590 33. Barber, M.F., Kronenberg, Z., Yandell, M., and Elde, N.C. (2016). Antimicrobial Functions of
591 Lactoferrin Promote Genetic Conflicts in Ancient Primates and Modern Humans. PLoS
592 Genet. *12*, e1006063.

593 34. Bridgham, J.T., Carroll, S.M., and Thornton, J.W. (2006). Evolution of hormone-receptor
594 complexity by molecular exploitation. Science *312*, 97–101.

595 35. Harms, M.J., and Thornton, J.W. (2010). Analyzing protein structure and function using
596 ancestral gene reconstruction. Curr. Opin. Struct. Biol. *20*, 360–366.

597 36. Starr, T.N., Picton, L.K., and Thornton, J.W. (2017). Alternative evolutionary histories in the
598 sequence space of an ancient protein. Nature *549*, 409–413.

599 37. Orlandi, K.N., Phillips, S.R., Sailer, Z.R., Harman, J.L., and Harms, M.J. (2023). Topiary:
600 Pruning the manual labor from ancestral sequence reconstruction. Protein Sci. *32*, e4551.

601 38. Letizia, M., Diggle, S.P., and Whiteley, M. (2025). Pseudomonas aeruginosa: ecology,
602 evolution, pathogenesis and antimicrobial susceptibility. Nat. Rev. Microbiol. *23*, 701–717.

603 39. Grace, A., Sahu, R., Owen, D.R., and Dennis, V.A. (2022). Pseudomonas aeruginosa
604 reference strains PAO1 and PA14: A genomic, phenotypic, and therapeutic review. Front.
605 Microbiol. *13*, 1023523.

606 40. Minogue, T.D., Daligault, H.A., Davenport, K.W., Bishop-Lilly, K.A., Broomall, S.M., Bruce,
607 D.C., Chain, P.S., Chertkov, O., Coyne, S.R., Freitas, T., et al. (2014). Complete genome

608 assembly of Escherichia coli ATCC 25922, a serotype O6 reference strain. Genome
609 Announc. *2*. https://doi.org/10.1128/genomeA.00969-14.

610 41. Cheung, G.Y.C., Bae, J.S., and Otto, M. (2021). Pathogenicity and virulence of
611 Staphylococcus aureus. Virulence *12*, 547–569.

612 42. Parsons, J.B., Mourad, A., Conlon, B.P., Kielian, T., and Fowler, V.G., Jr (2025). Methicillin-
613 resistant and susceptible Staphylococcus aureus: tolerance, immune evasion and treatment.
614 Nat. Rev. Microbiol. https://doi.org/10.1038/s41579-025-01226-2.

615 43. Maisey, H.C., Doran, K.S., and Nizet, V. (2008). Recent advances in understanding the
616 molecular basis of group B Streptococcus virulence. Expert Rev. Mol. Med. *10*, e27.

617 44. Cao, X., Ren, Y., Lu, Q., Wang, K., Wu, Y., Wang, Y., Zhang, Y., Cui, X.-S., Yang, Z., and
618 Chen, Z. (2022). Lactoferrin: A glycoprotein that plays an active role in human health. Front.
619 Nutr. *9*, 1018336.

620 45. Malanovic, N., Buttress, J.A., Vejzovic, D., Ön, A., Piller, P., Kolb, D., Lohner, K., and Strahl,
621 H. (2022). Disruption of the cytoplasmic membrane structure and barrier function underlies
622 the potent antiseptic activity of octenidine in Gram-positive bacteria. Appl. Environ. Microbiol.
623 *88*, e0018022.

624 46. Bhaumik, K.N., Spohn, R., Dunai, A., Daruka, L., Olajos, G., Zákány, F., Hetényi, A., Pál, C.,
625 and Martinek, T.A. (2024). Chemically diverse antimicrobial peptides induce
626 hyperpolarization of the E. coli membrane. Commun. Biol. *7*, 1264.

627 47. Lee, D.-Y.D., Galera-Laporta, L., Bialecka-Fornal, M., Moon, E.C., Shen, Z., Briggs, S.P.,
628 Garcia-Ojalvo, J., and Süel, G.M. (2019). Magnesium flux modulates ribosomes to increase
629 bacterial survival. Cell *177*, 352-360.e13.

630 48. Te Winkel, J.D., Gray, D.A., Seistrup, K.H., Hamoen, L.W., and Strahl, H. (2016). Analysis of
631 antimicrobial-triggered membrane depolarization using voltage sensitive dyes. Front. Cell
632 Dev. Biol. *4*, 29.

633 49. Chen, E.H.-L., Wang, C.-H., Liao, Y.-T., Chan, F.-Y., Kanaoka, Y., Uchihashi, T., Kato, K.,
634 Lai, L., Chang, Y.-W., Ho, M.-C., et al. (2023). Visualizing the membrane disruption action of
635 antimicrobial peptides by cryo-electron tomography. Nat. Commun. *14*, 5464.

636 50. Yang, Z., Choi, H., and Weisshaar, J.C. (2018). Melittin-induced permeabilization, re-
637 sealing, and re-permeabilization of E. coli membranes. Biophys. J. *114*, 368–379.

638 51. Rice, A., Zourou, A.C., Cotten, M.L., and Pastor, R.W. (2025). A unified model of transient
639 poration induced by antimicrobial peptides. Proc. Natl. Acad. Sci. U. S. A. *122*,
640 e2510294122.

641 52. Tam, K., and Torres, V.J. (2019). Staphylococcus aureus Secreted Toxins and Extracellular
642 Enzymes. Microbiol Spectr *7*. https://doi.org/10.1128/microbiolspec.GPP3-0039-2018.

643 53. Koymans, K.J., Vrieling, M., Gorham, R.D., Jr, and van Strijp, J.A.G. (2017). Staphylococcal
644 immune evasion proteins: Structure, function, and host adaptation. Curr. Top. Microbiol.
645 Immunol. *409*, 441–489.

646 54. Haag, A.F., Fitzgerald, J.R., and Penadés, J.R. (2019). Staphylococcus aureus in animals.
647 Microbiol. Spectr. *7*. https://doi.org/10.1128/microbiolspec.GPP3-0060-2019.

648 55. Antunes, B., Zanchi, C., Johnston, P.R., Maron, B., Witzany, C., Regoes, R.R., Hayouka, Z.,
649 and Rolff, J. (2024). The evolution of antimicrobial peptide resistance in Pseudomonas
650 aeruginosa is severely constrained by random peptide mixtures. PLoS Biol. *22*, e3002692.

651 56. Unckless, R.L., Howick, V.M., and Lazzaro, B.P. (2016). Convergent Balancing Selection on
652 an Antimicrobial Peptide in Drosophila. CURBIO *26*, 257–262.

653 57. van Dijk, A., Guabiraba, R., Bailleul, G., Schouler, C., Haagsman, H.P., and Lalmanach, A.-
654 C. (2023). Evolutionary diversification of defensins and cathelicidins in birds and primates.
655 Mol. Immunol. *157*, 53–69.

656 58. Geiger, R.A., Khera, D., Tenthorey, J.L., Kochs, G., Graf, L., Emerman, M., and Malik, H.S.
657 (2025). Heterozygous and generalist MxA super-restrictors overcome breadth-specificity
658 trade-offs in antiviral restriction. Sci. Adv. *11*, eadu0062.

659 59. Cheng, K.J., Shastry, S., Campolargo, J.D., Hallock, M.J., and Pogorelov, T.V. (2025).
660 Charge, hydrophobicity, and lipid type drive antimicrobial peptides' unique perturbation
661 ensembles. Biochemistry *64*, 1484–1500.

662 60. van der Kraan, M.I.A., Groenink, J., Nazmi, K., Veerman, E.C.I., Bolscher, J.G.M., and
663 Nieuw Amerongen, A.V. (2004). Lactoferrampin: a novel antimicrobial peptide in the N1-
664 domain of bovine lactoferrin. Peptides *25*, 177–183.

665 61. Ibrahim, H.R., Iwamori, E., Sugimoto, Y., and Aoki, T. (1998). Identification of a distinct
666 antibacterial domain within the N-lobe of ovotransferrin. Biochim. Biophys. Acta *1401*, 289–
667 303.

668 62. Rathnapala, E.C.N., Ahn, D.U., and Abeyrathne, S. (2021). Functional properties of
669 ovotransferrin from chicken egg white and its derived peptides: a review. Food Sci.
670 Biotechnol. *30*, 619–630.

671 63. Hanson, M.A., Hamilton, P.T., and Perlman, S.J. (2016). Immune genes and divergent
672 antimicrobial peptides in flies of the subgenus Drosophila. BMC Evol. Biol. *16*, 228.

673 64. Chapman, J.R., Hill, T., and Unckless, R.L. (2019). Balancing selection drives the
674 maintenance of genetic variation in Drosophila antimicrobial peptides. Genome Biol. Evol.
675 *11*, 2691–2701.

676 65. Hanson, M.A., Grollmus, L., and Lemaitre, B. (2023). Ecology-relevant bacteria drive the
677 evolution of host antimicrobial peptides in Drosophila. Science *381*, eadg5725.

678 66. Mirdita, M., Schütze, K., Moriwaki, Y., Heo, L., Ovchinnikov, S., and Steinegger, M. (2022).
679 ColabFold: making protein folding accessible to all. Nat. Methods *19*, 679–682.

680 67. Pettersen, E.F., Goddard, T.D., Huang, C.C., Couch, G.S., Greenblatt, D.M., Meng, E.C.,
681 and Ferrin, T.E. (2004). UCSF Chimera--a visualization system for exploratory research and
682 analysis. J. Comput. Chem. *25*, 1605–1612.

683 68. Gasteiger, E., Hoogland, C., Gattiker, A., Duvaud, S., Wilkins, M.R., Appel, R.D., and
684 Bairoch, A. (2005). Protein identification and analysis tools on the ExPASy server. In The
685 Proteomics Protocols Handbook (Humana Press), pp. 571–607.

686 69. Dombach, J.L., Quintana, J.L.J., and Detweiler, C.S. (2021). Staphylococcal bacterial
687 persister cells, biofilms, and intracellular infection are disrupted by JD1, a membrane-
688 damaging small molecule. MBio *12*, e0180121.

70. Schindelin, J., Arganda-Carreras, I., Frise, E., Kaynig, V., Longair, M., Pietzsch, T., Preibisch, S., Rueden, C., Saalfeld, S., Schmid, B., et al. (2012). Fiji: an open-source platform for biological-image analysis. Nat. Methods *9*, 676–682.

71. Greco, I., Molchanova, N., Holmedal, E., Jenssen, H., Hummel, B.D., Watts, J.L., Håkansson, J., Hansen, P.R., and Svenson, J. (2020). Correlation between hemolytic activity, cytotoxicity and systemic in vivo toxicity of synthetic antimicrobial peptides. Sci. Rep. *10*, 13206.

697 **Figures**

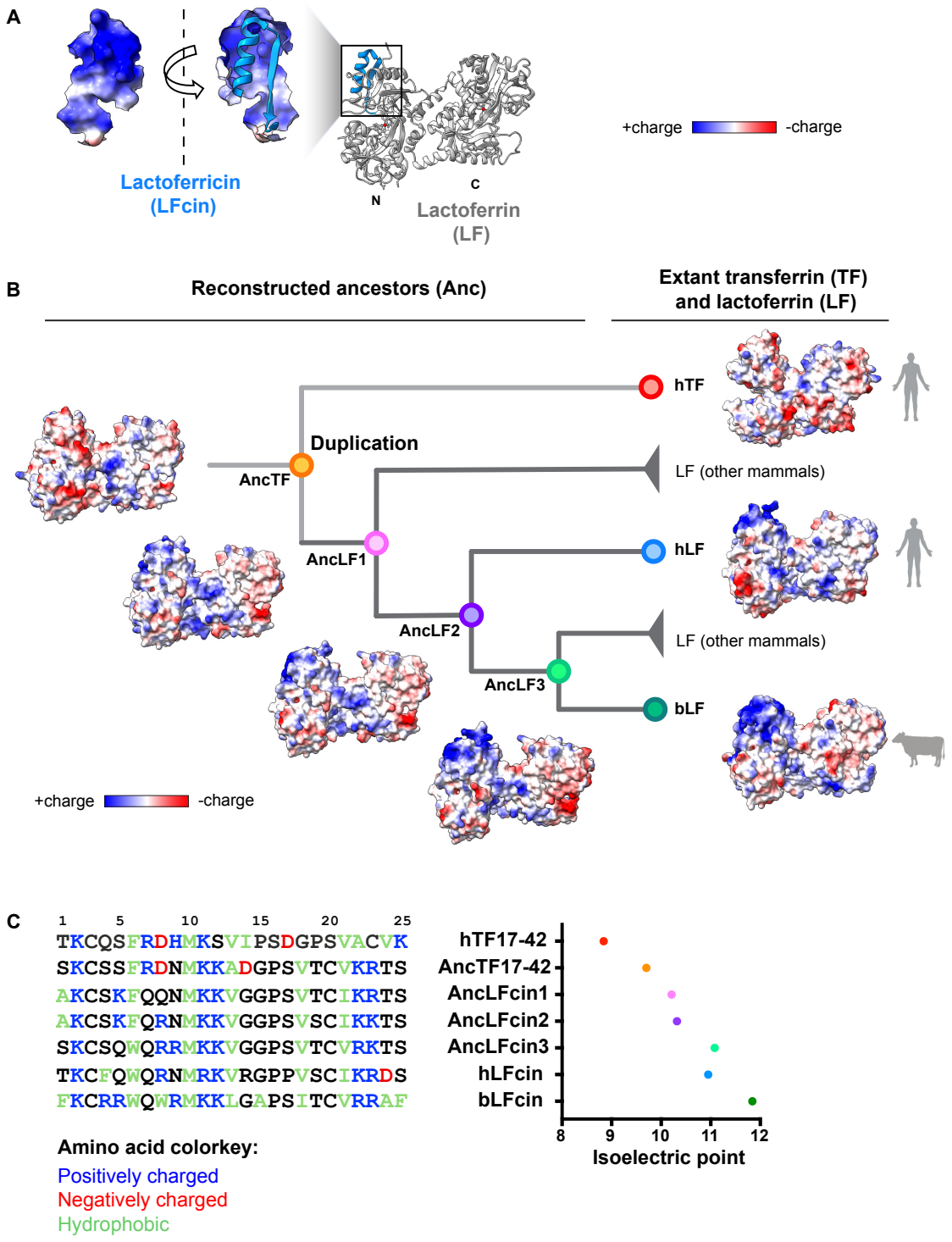

698
699 **Figure 1. Retracing the emergence of antimicrobial function in mammalian lactoferrin.** (**A**)
700 Structure of the N-terminal lactoferricin region of lactoferrin (PDB: 1lfg), enriched with positively
701 charged amino acids. (**B**) Phylogenetic tree of reconstructed ancestral lactoferrin homologs
702 (AncTF and AncLF) with extant human transferrin (hTF, PDB: 3qyt), human lactoferrin (hLF, PDB:

703 1lfg), and bovine lactoferrin (bLF, PDB: 1blf) illustrated with surface electrostatic potentials.
704 Structures of ancestral proteins were predicted using AlphaFold2. AncTF represents the last
705 common ancestor of mammalian transferrin and lactoferrin, after which the first lactoferrin
706 ancestor (AncLF1) arose by gene duplication. AncLF2 is the common ancestor of hLF and bLF,
707 while AncLF3 represents a bLF ancestor. (**C**) Alignment of the lactoferricin region from hTF,
708 AncTF, selected AncLFs, hLF, and bLF, with their corresponding isoelectric points. Higher
709 isoelectric points indicate higher incidence of positive charges.
710

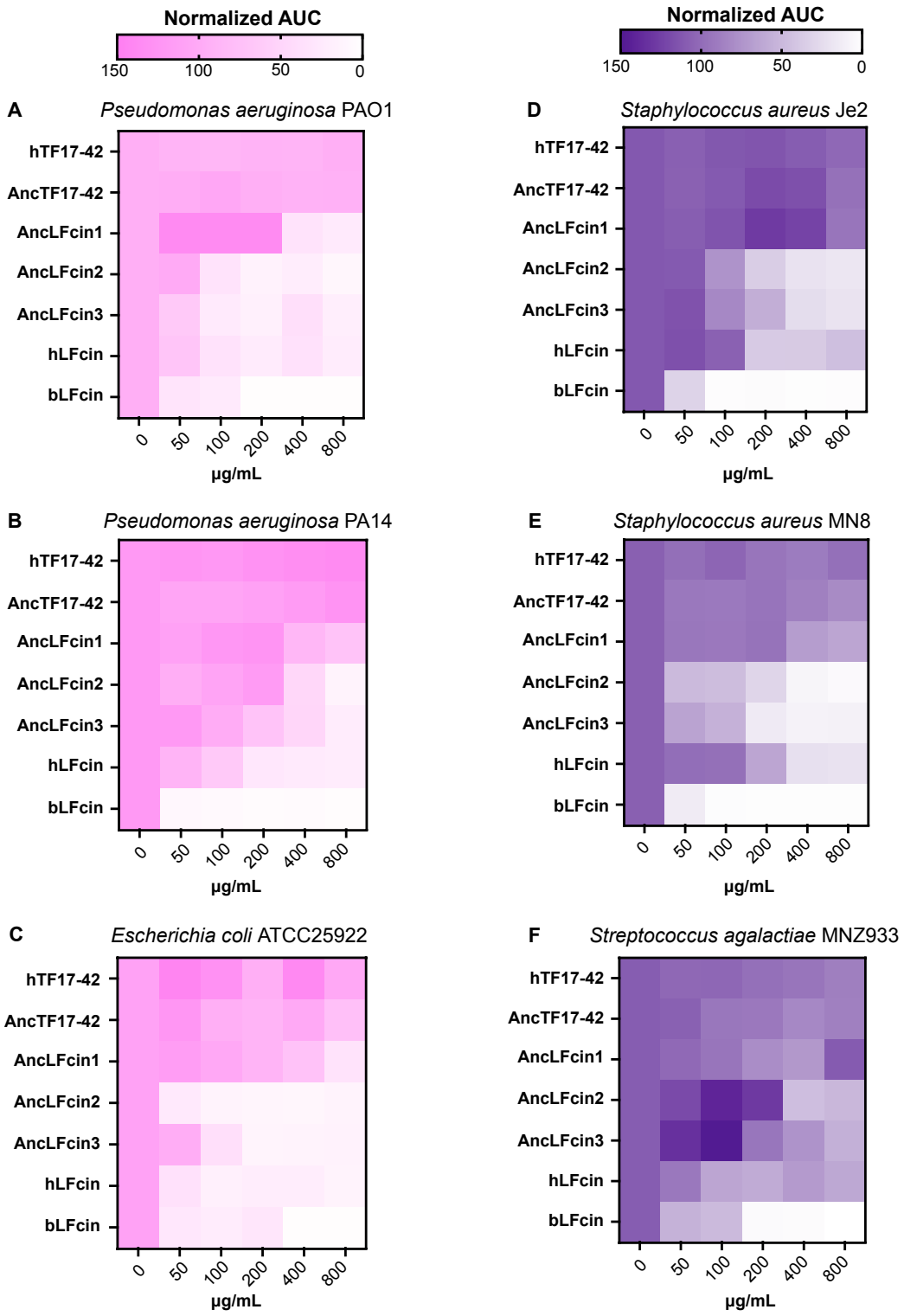

Figure 2. origin of antimicrobial activity in lactoferricin. Heatmaps depict area under the curve (AUC) values normalized against the untreated control from bacterial growth curves performed in the presence of indicated peptides at specified concentrations. Gram-negative strains are shown in pink (A-C), Gram-positive strains in purple (D-F).

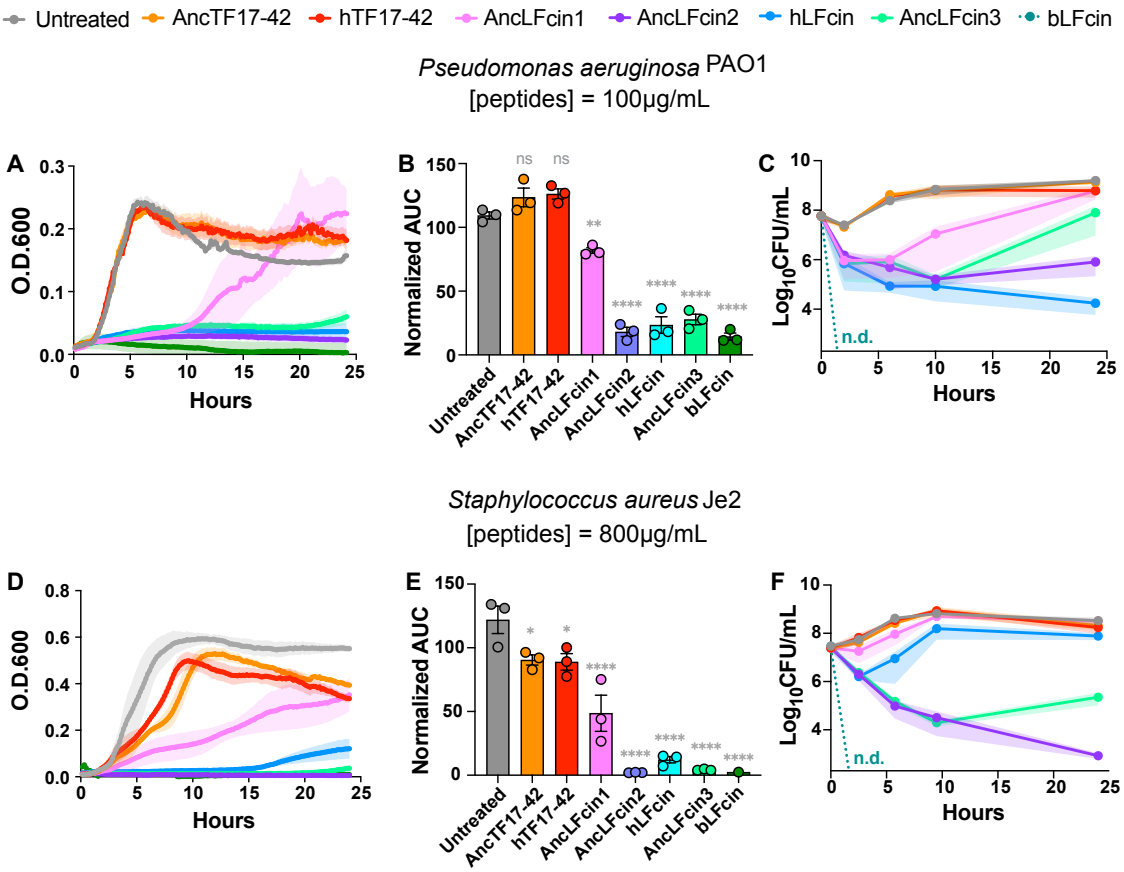

Figure 3. Stepwise evolution of bactericidal activity in ancestral lactoferricin. (**A-C**) *Pseudomonas aeruginosa* strain PAO1 treated with 100 µg/mL of indicated peptides, (**D-F**) *Staphylococcus aureus* strain JE2 treated with 800 µg/mL of indicated peptides. (**A, D**) Growth curves measured by optical density at 600 nm over time. (**B, E**) Corresponding area under the curve (AUC) measurements normalized against untreated control based on bacterial growth curves. (**C, F**) Bacterial survival curves measured as colony forming units (CFUs). All data represent mean and standard error based on three biological replicates. Statistical significance was determined using one-way ANOVA (*$P \leq 0.05$, **$P \leq 0.01$, ***$P \leq 0.001$, ****$P \leq 0.0001$; ns, not significant).

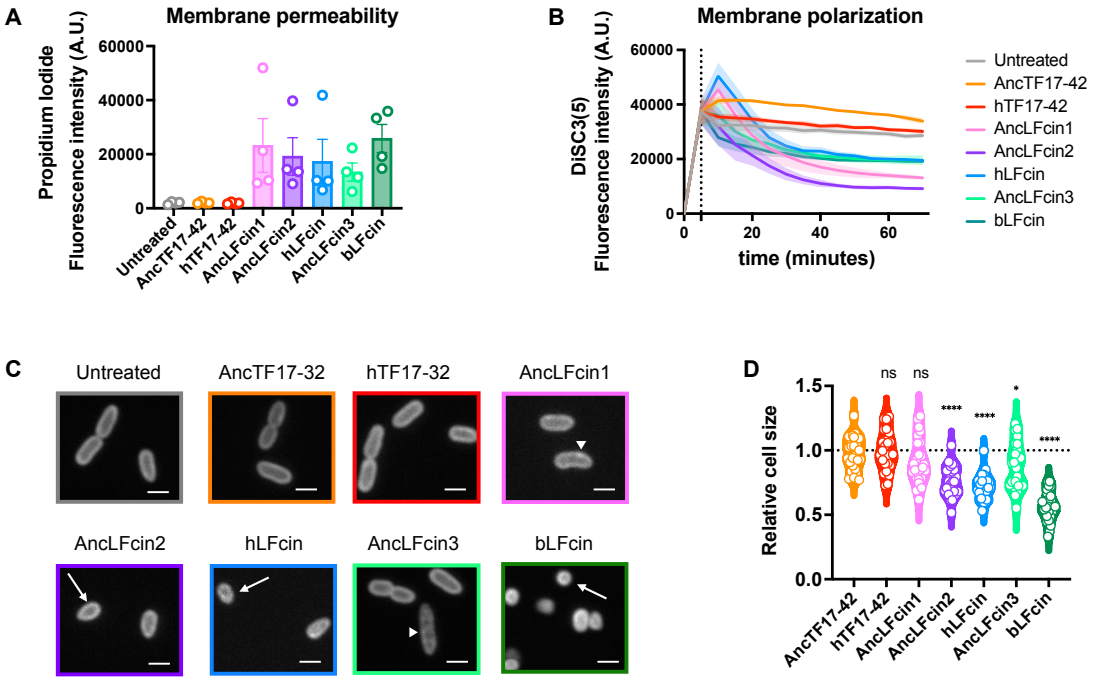

Figure 4. Lactoferricin membrane permeabilizing activity emerged early after gene duplication. *Pseudomonas aeruginosa* strain PAO1 was treated with 100 µg/mL of indicated peptides for 30-60 minutes to assess membrane disruption and cell morphology. (**A**) Membrane permeabilization measured by propidium iodide staining after 30 minutes of treatment. (**B**) Membrane polarization measured by DiSC3(5) dye after 1 hour of treatment. Peptides were added 5 minutes after addition of the dye (shown with the dotted line). Lower fluorescence indicates hyperpolarization. Data represent mean and standard error based on three biological replicates. (**C**) Confocal microscopy images of peptide-treated cells at 30 minutes (scale bar, 1µM). (**D**) Quantification of bacterial cell size from microscopy images (n=100). Statistical significance was determined using one-way ANOVA (*$P \leq 0.05$, **$P \leq 0.01$, ***$P \leq 0.001$, ****$P \leq 0.0001$; ns, not significant).

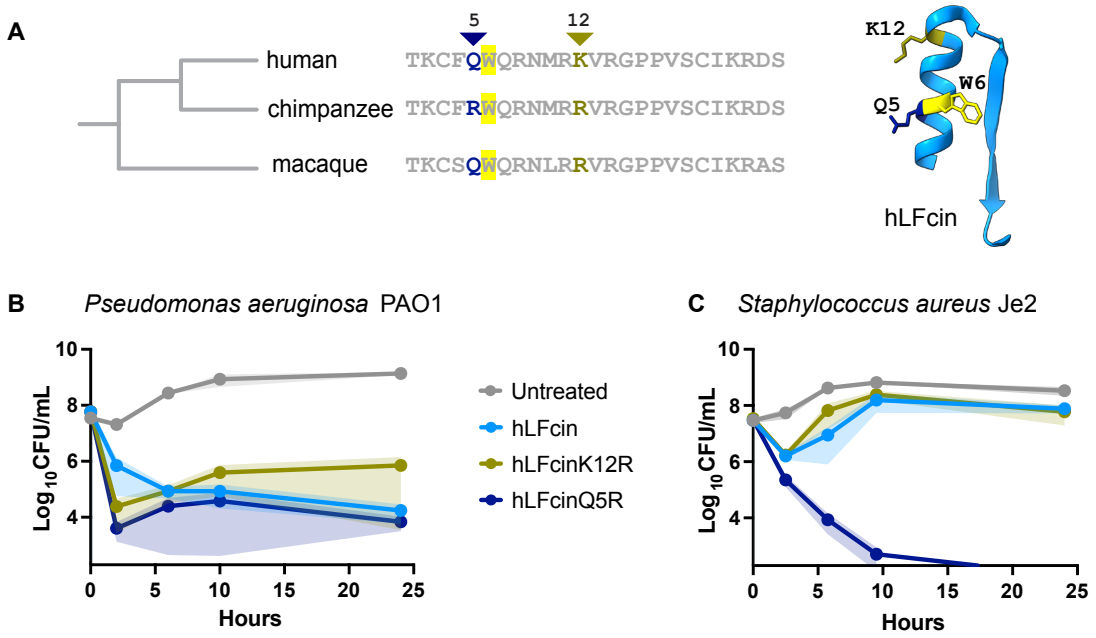

Figure 5. Natural selection enhanced lactoferricin antimicrobial potency in great apes. (A) Alignment of lactoferricin orthologs from humans, chimpanzees, and rhesus macaques. Two sites (positions 5 and 12) exhibit elevated dN/dS across primates. (B) Antimicrobial activity of hLFcin and mutant peptides against *Pseudomonas aeruginosa* PAO1 at 100 µg/mL. (C) Antimicrobial activity of hLFcin and mutant peptides against *Staphylococcus aureus* strain JE2 at 800 µg/mL. Data represent mean and standard error based on three biological replicates.